

QUOTA: Quantifying Objects with Text-to-Image Models for Any Domain

Wenfang Sun^{1*}, Yingjun Du^{2*}, Gaowen Liu³, Cees G. M. Snoek²

¹University of Science and Technology of China ²University of Amsterdam

³Cisco Research

Abstract

We tackle the problem of quantifying the number of objects by a generative text-to-image model. Rather than re-training such a model for each new image domain of interest, which leads to high computational costs and limited scalability, we are the first to consider this problem from a domain-agnostic perspective. We propose QUOTA, an optimization framework for text-to-image models that enables effective object quantification across unseen domains without retraining. It leverages a dual-loop meta-learning strategy to optimize a domain-invariant prompt. Further, by integrating prompt learning with learnable counting and domain tokens, our method captures stylistic variations and maintains accuracy, even for object classes not encountered during training. For evaluation, we adopt a new benchmark specifically designed for object quantification in domain generalization, enabling rigorous assessment of object quantification accuracy and adaptability across unseen domains in text-to-image generation. Extensive experiments demonstrate that QUOTA outperforms conventional models in both object quantification accuracy and semantic consistency, setting a new benchmark for efficient and scalable text-to-image generation for any domain.

1. Introduction

Text-to-image generative models [7, 40, 57, 67] have achieved remarkable success in generating high-quality images from textual descriptions. However, accurately controlling the count of objects in these generated images remains challenging, particularly when faced with text prompts that embody domains different from the ones seen during training. Recently, Zafar *et al.* [66] introduce prompt learning to refine the object counting prompts. While effective in controlled scenarios, this method struggles to maintain accurate object counts when confronted with varying domains. As a result, achieving domain-generalizable object quantification remains a crucial and unresolved challenge across various

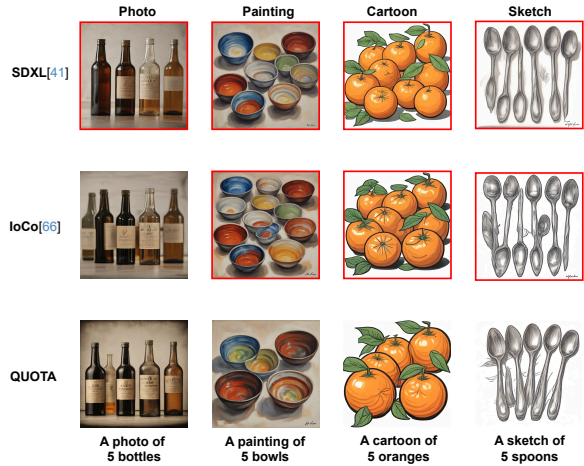


Figure 1. Quantifying objects for any domain. The images outlined in red represent cases where the generated images have incorrect object counts. SDXL [41] struggles to control object counts across various domains, demonstrating inconsistencies even in domains typically encountered during training. IoCo by Zafar *et al.* [66], trained specifically on the photo domain, also faces challenges in generalizing object quantification to unseen styles. Our proposed QUOTA method achieves consistent and accurate object quantification for any domain.

generative models, including diffusion and flow-matching models. Figure 1 illustrates this issue, showing how standard generative models like SDXL [41] struggle with accurate object quantification across different domains, whereas our approach provides consistent and accurate results across diverse domains.

Domain generalization in machine learning aims to create models that perform well on unseen domains, reducing the need for retraining and enabling greater adaptability across diverse settings. A wide range of approaches has been developed for this purpose, including methods that focus on learning domain-invariant features and leveraging diverse training environments [9, 31, 63]. Among these approaches, meta-learning has emerged as a promising technique, enabling models to adapt to new tasks by utilizing prior knowledge

*Equal contribution.

from related tasks [12, 20, 60]. Meta-learning has demonstrated success in improving domain generalization across various applications by optimizing models to adapt to different scenarios. Despite these advancements, there has been no exploration of meta-learning for domain-generalizable object quantification in text-to-image generation. In this paper, we fill this gap by proposing a novel meta-learning framework specifically designed to enable robust object quantification across diverse and unseen domains within text-to-image models.

Specifically, we make the following three contributions in this paper. *First*, we introduce a domain-agnostic setting for object quantification in generative text-to-image models, emphasizing the need for precise, domain-invariant object quantification across domains. This setting is essential for adapting models to diverse and unseen prompts without retraining, addressing both scalability and efficiency challenges. *Second*, we propose a dual-loop meta-learning strategy for prompt optimization, designed to make prompts domain-invariant. In the training phase, we divide text prompts into meta-train and meta-test domains. In the inner loop, we optimize prompt parameters on the meta-train domain to meet specific domain requirements. The outer loop refines these parameters on the meta-test domain, allowing the model to learn a prompt that generalizes across unseen domains. *Third*, we incorporate prompt learning with learnable quantification and domain tokens, enabling the model to capture stylistic variations effectively while preserving object quantification accuracy across domains. This approach allows for robust adaptation to new domains and unseen object classes without modifying the model architecture or retraining.

For evaluation, we adopt a new benchmark specifically designed for object quantification in domain generalization, enabling rigorous assessment of accuracy and adaptability across unseen domains in text-to-image generation.

Comparative evaluations against state-of-the-art methods demonstrate that QUOTA outperforms existing models in both object quantification accuracy and semantic alignment, setting a new benchmark for efficient, adaptable, and scalable text-to-image generation.

2. Related Work

The field of image generation has seen extensive study, from early advancements with GANs [15, 30, 34, 42, 43, 59, 68] to recent breakthroughs with diffusion models [6, 13, 19, 24, 45]. Diffusion models, in particular, have unlocked remarkable capabilities for generating high-quality, diverse images directly from natural language descriptions, exemplified by models like DALL-E 2 [46], Imagen [51], Parti [65], Make-A-Scene [13], Stable Diffusion (SD) [49], and CogView2 [8]. Our method builds on text-conditioned image generation, specifically exploring how to enhance object counting consistency across domains. Below, we review related areas in

editing and controlling image generation models.

Personalized Image Generation. Personalization in image generation typically focuses on fine-tuning models to represent specific concepts from limited examples. Textual Inversion [14], for instance, learns a new token to represent a concept using just 3-5 images, while DreamBooth [50] fine-tunes diffusion model parameters. However, adapting models to represent quantitative concepts, such as object counts, poses unique challenges as it involves precise numeric representation rather than qualitative identity. In contrast, our work focuses on achieving precise, domain-generalizable object quantification across varied styles and contexts without retraining, extending personalized image generation to handle quantitative control across different visual styles and settings.

Optimizing Prompt Correspondence. Recent studies have improved the alignment between text prompts and generated images. Prompt-to-Prompt [17] manipulates textual encoder attention for object replacement, while Null-inversion [36] allows similar edits on real images. Attend-and-Excite [5] ensures all objects in a prompt are depicted by optimizing attention maps. However, these methods generally do not address numeric accuracy in object counts, as prompt manipulation alone often fails to ensure precise quantities in diffusion outputs. Our work addresses this gap by introducing meta-optimized prompts that enable reliable control over object quantities across varied styles and contexts, establishing a foundation for robust object quantification in diverse visual settings.

Domain Generalization. Domain generalization (DG) aims to learn knowledge that transfers well to unseen target domains, allowing models to generalize effectively without access to target domain data during training. DG is typically studied under two main settings: multi-source domain generalization and single domain generalization (SDG). Multi-source DG utilizes multiple source domains to enhance robustness, while SDG—considered more realistic yet challenging—relies on a single source domain, making it harder due to limited data diversity. Early approaches to DG drew inspiration from domain adaptation methods, focusing on domain alignment to learn domain-invariant features. Techniques such as adversarial training [25, 53] and distribution distance minimization [32, 33] were employed to reduce feature bias across multiple source domains. Additionally, self-supervised learning [4, 26] and meta-learning [9, 55] have been explored to improve generalization in DG tasks. However, to the best of our knowledge, no prior work has specifically addressed domain-generalizable object quantification in text-to-image diffusion models. Our work introduces a novel setting and methodology to achieve domain-invariant object quantification across diverse and unseen domains. This new setting expands the scope of domain generalization research to the area of text-to-image generation,

where accurate object quantification across varied domains is crucial.

Meta-Learning. Meta-learning, or learning to learn, seeks to enable rapid and efficient adaptation to new tasks by leveraging prior learning experiences, as reviewed by Hospedales *et al.* [21]. It has been applied across diverse areas, including designing adaptive loss functions [2, 3, 54], creating task-specific model initializations [12], and advancing few-shot learning techniques [9, 10, 28, 56, 58]. Meta-learning approaches are generally categorized into metric-based [29, 56, 58, 61], memory-based [11, 20, 35, 37, 38, 52], and gradient-based methods [16, 31, 39, 48]. Since the introduction of Model-Agnostic Meta-Learning (MAML) [12], gradient-based approaches have gained popularity, though they often encounter challenges with meta-overfitting due to limited meta-training tasks [1, 22, 23, 27, 64, 69]. Overall, meta-learning serves as a crucial foundation for our approach, enabling effective domain generalization in object quantification by facilitating adaptive prompt optimization across diverse text-to-image generation tasks.

3. Preliminaries

Text-Conditioned Diffusion Process. The diffusion process generates an image $x \sim p(x)$ from random noise through an iterative denoising procedure. Given an image $x_0 \sim p(x)$, training involves creating noisy samples $x_t = \sqrt{\alpha_t}x_0 + \sqrt{1 - \alpha_t}\epsilon_t$, where α_t are hyperparameters and $\epsilon_t \sim \mathcal{N}(0, I)$. A neural network is trained to predict the added noise ϵ_t using the following objective:

$$\mathbb{E}_{x, \epsilon_t, t} [\|\hat{\epsilon}_\theta(x_t, t) - \epsilon_t\|_2^2]. \quad (1)$$

For conditional denoising, a similar objective is applied, with each step conditioned on an external factor y :

$$\mathbb{E}_{x, \epsilon_t, t} [\|\hat{\epsilon}_\theta(x_t, t, y) - \epsilon_t\|_2^2]. \quad (2)$$

In text-to-image diffusion, training involves reconstructing images conditioned on textual descriptions, which guide the denoising process to match the text. This requires a large dataset to generalize mappings between text and object quantities accurately. Some approaches modify noise predictions to align with specific object counts [66], although these often require counting models capable of handling noisy, intermediate data. In our work, we propose a method that adjusts the text conditioning embeddings using feedback from an off-the-shelf counting model.

Meta-Learning. Meta-learning aims to build models capable of quickly adapting to new tasks with limited data by utilizing prior experiences across various tasks [12]. Let \mathcal{D} represent a meta-training dataset composed of training and validation sets across a range of tasks \mathcal{T} , i.e., $\mathcal{D} = \{\{D_i^{\text{tr}}, D_i^{\text{val}}\}\}_{i \in \mathcal{T}}$, where D_i^{tr} and D_i^{val} are the training and validation datasets for the i -th task. Meta-learning

can be formulated as a bi-level optimization problem:

$$\min_{\phi} \sum_{i \in \mathcal{T}} \mathcal{L}_{\text{val}}(\hat{\theta}_i(\phi); D_i^{\text{val}}) \quad (3)$$

$$\text{s.t. } \hat{\theta}_i(\phi) = \arg \min_{\theta_i} \mathcal{L}_{\text{train}}(\theta_i; \phi, D_i^{\text{tr}}), \forall i \in \mathcal{T}, \quad (4)$$

where \mathcal{L}_{val} and $\mathcal{L}_{\text{train}}$ represent the validation and training losses for the upper- and lower-level optimizations, respectively. In this setup, θ_i denotes the task-specific parameters for the i -th task, while ϕ are the meta-parameters shared across tasks. The lower-level optimization (Eq. (4)) adapts task-specific parameters θ_i for each task using the meta-parameters ϕ and the task-specific training set D_i^{tr} . Meanwhile, the upper-level optimization (Eq. (3)) aims to find meta-parameters ϕ that minimize the aggregated validation loss across tasks based on the optimized task-specific parameters $\hat{\theta}_i(\phi)$. Our work leverages this meta-learning framework to achieve domain-generalizable object quantification in text-to-image diffusion models, employing a dual-loop optimization approach to refine style-invariant prompts across diverse domains.

4. Methods

In this section, we introduce quantifying objects with text-to-image models for any domain (QUOTA), our approach for quantifying object quantities across diverse domains in text-to-image generative models. QUOTA leverages a dual-loop meta-learning framework to create domain-invariant prompts that guide object quantification without retraining, making it adaptable to new and unseen domains. Through prompt learning, QUOTA optimizes domain-specific and quantity-specific parameters to accurately adjust object quantities based on textual prompts, even when encountering new stylistic variations. Our framework operates on images generated by existing text-to-image models, such as SDXL [41], using object quantities inferred by a pre-trained detection model as feedback for optimization.

4.1. Domain-generalizable object quantification

Accurately controlling the quantity of objects in text-to-image generative models is essential for producing realistic images, especially when adapting to diverse domains. To address the challenge of domain generalization, we introduce a novel training framework where multiple domains are leveraged to optimize the text-to-image generation process for consistent object quantification. Let $\mathcal{D} = \{\mathcal{D}_{\text{train}}, \mathcal{D}_{\text{test}}\}$ represent the set of domains available in the training phase, where $\mathcal{D}_{\text{train}}$ denotes the meta-train domains and $\mathcal{D}_{\text{test}}$ represents a held-out meta-test domain. During each iteration, we randomly select one domain from the training domains as the meta-test domain $\mathcal{D}_{\text{test}}$, while the remaining domains are assigned as the meta-train domains $\mathcal{D}_{\text{train}}$. This randomized

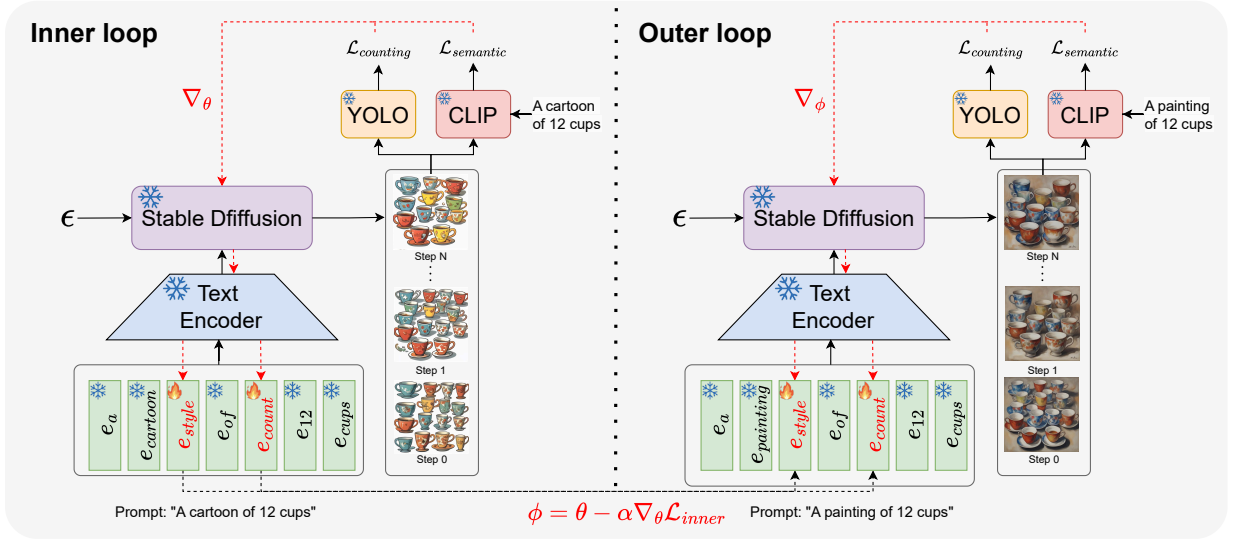


Figure 2. QUOTA’s dual-loop meta-optimization. The inner loop optimizes prompt parameters e_{count} and e_{style} across meta-train domains to adapt to domain-specific prompts, with losses computed using YOLOv9 for quantification accuracy and CLIP for semantic alignment. The outer loop refines these parameters on a meta-test domain, enhancing the model’s generalization to unseen domains. This dual-loop structure enables consistent object quantification and domain adaptation across diverse domains without the need for retraining.

selection allows the model to experience different combinations of training and testing domains, enhancing its robustness and adaptability to unseen domains. During training, images are generated based on text prompts in each domain using a pre-trained diffusion model, such as SDXL [41], without access to ground truth images. This setting enables us to simulate diverse training scenarios, preparing the model for domain shifts.

In the testing phase, our goal is to generalize to an unseen domain $\mathcal{D}_{\text{unseen}}$, where the model is expected to quantify objects accurately in images generated by the text-to-image model. To evaluate the object counts in these generated images, we employ two pre-trained models: YOLOv9 [62] and CLIP-S [44]. YOLOv9 serves as an object detector, providing a quantitative measure of the number of objects present in the image. Meanwhile, CLIP-S offers an alignment score between the generated image and the text prompt, helping to assess how well the generated image adheres to the prompt’s specifications, including object count. Notably, since the diffusion process does not inherently support direct control over object counts, we rely on a pre-trained object counting model that operates on completed images rather than intervening in the intermediate denoising steps. Thus, our method focuses on refining the domain and quantification parameters of the prompt, allowing it to adapt to the generated image characteristics across various domains and ensure accurate quantify object in the final output.

4.2. Dual-loop meta-optimization

QUOTA leverages a dual-loop meta-learning approach to achieve domain-invariant object quantification across diverse domains. This process involves an inner loop, which adapts the prompt parameters across multiple meta-train domains, and an outer loop, which refines these parameters on a single meta-test domain to encourage domain generalization. Each loop’s loss function incorporates two components: a quantification loss for object accuracy and a CLIP matching penalty to maintain semantic consistency. See Figure 2 for an overview.

Inner loop optimization. In the inner loop, given a set of meta-train domains $\mathcal{D}_{\text{train}}$, we optimize the prompt parameters θ across multiple domains to ensure the adaptability of the model. For each domain $d \in \mathcal{D}_{\text{train}}$, the composite loss function includes:

Quantification loss. Our inner loop optimization process utilizes a differentiable counting function, Count , which estimates the quantity of objects for a specified class in an image. The quantification loss for a target class c is defined as the difference between the estimated and desired object counts, given by:

$$\mathcal{L}_{\text{counting}}(x_d, c, N) = \|\text{Count}(x_d, c) - N\|, \quad (5)$$

where $\text{Count}(x_d, c)$ provides an estimate of the object count for class c within the generated image x_d . This loss is calculated using a detection-based dynamic scale, leveraging YOLOv9 [62] to estimate the count of objects of class c in the generated image x_d . The estimated count is given by:

$$\text{Count}(x_d, c) = \sum_{i=1}^{h \cdot w} \hat{\lambda}_{\text{scale}, x_d, \mathcal{D}} \cdot \Phi_i(x_d, c), \quad (6)$$

where $\hat{\lambda}_{\text{scale}, x_d}$ is a dynamically adjusted scaling factor for differentiation continuity, and $\Phi_i(x_d, c)$ represents the detection score for class c at each pixel. This loss penalizes the difference between the target count N and the detected count, ensuring accurate object quantification.

CLIP matching penalty. To ensure the image semantics remain intact, we add a CLIP-based penalty term:

$$\mathcal{L}_{\text{semantic}}(x_d, c; \theta) = \text{CLIP}(x_d, \text{“A } s_d \text{ of } c\text{”}), \quad (7)$$

where s_d is a domain descriptor specific to the domain d (e.g., “photo,” “sketch,” “cartoon,” or “painting”), and CLIP provides a matching score between the generated image x_d and the textual description “A [style] of [class],” reinforcing both semantic and stylistic alignment.

The inner loop loss $\mathcal{L}_{\text{inner}}$ is then computed by summing these losses across all meta-train domains:

$$\mathcal{L}_{\text{inner}}(\theta) = \sum_{d \in \mathcal{D}_{\text{train}}} \mathcal{L}_{\text{counting}}(x_d, c, N; \theta) + \lambda \mathcal{L}_{\text{semantic}}(x_d, c; \theta), \quad (8)$$

where λ is a hyperparameter balancing the importance of object quantification accuracy and semantic consistency. This inner loop optimization updates the prompt parameters θ to adapt to the specific characteristics of the meta-train domains.

Outer loop optimization. The outer loop further refines the prompt parameters by evaluating them on the meta-test domain $\mathcal{D}_{\text{test}}$ to promote generalization to unseen domains. After optimizing the prompt parameters θ in the inner loop across meta-train domains, the outer loop computes the loss on the meta-test domain, defined as:

$$\mathcal{L}_{\text{outer}}(\phi) = \mathcal{L}_{\text{counting}}(x_{\text{test}}, c, N; \theta) + \lambda \mathcal{L}_{\text{semantic}}(x_{\text{test}}, c; \theta), \quad (9)$$

where x_{test} is the generated image using the updated prompt parameters θ from the inner loop on the meta-test domain $\mathcal{D}_{\text{test}}$, and ϕ represents the global meta-parameters. This outer optimization step updates ϕ , ensuring that the learned prompt parameters are robust enough to generalize to new, unseen domains, achieving accurate object quantification while maintaining semantic fidelity.

Through this dual-loop meta-optimization framework, QUOTA adapts the prompt parameters to handle domain shifts effectively, enabling consistent object quantification across various domains without compromising image quality or semantic alignment.

4.3. Learnable quantification and domain tokens

To achieve adaptive control over both object quantification and domain in text-to-image generation, we introduce prompt learning with two learnable tokens, e_{count} and e_{style} . These tokens enable the model to flexibly adjust to different domains while maintaining accurate object quantification. This approach enhances the model’s ability to generalize across diverse domains by encoding information specific to object quantification and stylistic features directly within the prompt. Notably, all other model parameters remain fixed, allowing the model to achieve domain adaptability without altering the underlying architecture.

The process starts with an initial prompt format: “A s_d of N c ,” where s_d represents the domain (e.g., “photo,” “sketch,” “cartoon”), N specifies the target object count, and c denotes the object class. To exercise control over the generated image, we concatenate two newly added pseudo token embeddings, e_{count} and e_{style} , to the text embedding. These embeddings are randomly initialized and are iteratively updated during training to adaptively encode information about object quantification and domain.

Unlike optimizing existing tokens, which may corrupt tokens with multiple meanings or associations, the introduction of these pseudo tokens allows the model to learn domain-specific adjustments without impacting predefined tokens. Formally, we optimize the embeddings e_{count} and e_{style} for each image generated, where the prompt parameters θ in our meta-optimization framework refer to these learnable tokens. In the inner loop, e_{count} and e_{style} are trained across meta-train domains to capture domain-specific prompt characteristics, resulting in domain-specific embeddings. The outer loop then refines these embeddings by adjusting the meta-parameters to generalize across domains, using the meta-test domain to guide the final optimization. The outer loop’s updated meta-parameters represent our optimized, domain-generalizable prompt embeddings, ensuring consistency in object quantification and domain adaptation even for unseen domains.

4.4. Testing phase

During testing on a new domain, we simply incorporate the domain and quantification information from the test text prompt by concatenating it with our learned tokens, e_{style} and e_{count} . For example, if the input text prompt is “a cartoon of 6 apples,” the prompt fed to SDXL [41] becomes “a cartoon e_{style} of 6 e_{count} apples.” This approach allows us to generate images accurately aligned with the desired domain and object count without needing to re-optimize e_{style} and e_{count} , thus saving time and ensuring efficient adaptation to new domains.

	Photo		Painting		Cartoon		Sketch		Average						
	YOLO		CLIP-S \uparrow		YOLO		CLIP-S \uparrow		YOLO		CLIP-S \uparrow				
	MAE \downarrow	RMSE \downarrow			MAE \downarrow	RMSE \downarrow	MAE \downarrow	RMSE \downarrow	MAE \downarrow	RMSE \downarrow	MAE \downarrow	RMSE \downarrow			
w/o Meta-optimization	12.75	16.75	73.2	10.40	13.78	74.0	11.49	13.28	73.1	11.33	12.92	71.9	11.49	14.18	73.1
w/ Meta-optimization	10.09	13.98	74.3	8.04	11.04	75.9	9.48	11.92	74.8	9.15	11.69	74.1	9.19	12.16	74.8

Table 1. Impact of dual-Loop meta-optimization on object quantification and semantic alignment across different domains on the FSC benchmark. Lower values for MAE and RMSE indicate better counting accuracy, while higher CLIP-S scores represent better alignment with prompt semantics. Meta-optimization shows improvements across all metrics, especially in challenging domains such as Sketch, demonstrating its effectiveness in enhancing both object quantification and domain generalization.

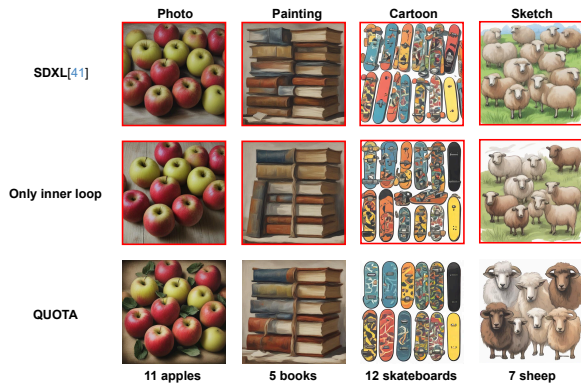


Figure 3. Comparison of object quantification results across domains with different optimization settings. This figure illustrates object quantification performance across various styles for three methods: SDXL [41], using only the inner loop in our framework, and our full QUOTA framework. The examples demonstrate how SDXL and the inner-loop-only setting struggle to achieve accurate quantification across domains, while meta-optimization achieves precise and consistent object quantification.

5. Experiments

5.1. Experimental setup

Benchmark. We developed *QUANT-Bench* to assess object quantification performance across various classes, quantities, and visual domains. The classes in *QUANT-Bench* are based on the FSC dataset [47], a widely used dataset for object quantification that includes 19 categories such as common objects, vehicles, and animals. For each class, we generated 25 examples for quantities ranging from one to 25, yielding a total of 475 samples. To evaluate the model’s ability to generalize across different domains, we created images in four distinct domains: *Photo*, *Painting*, *Cartoon*, and *Sketch*. Both training and testing categories are drawn from the FSC dataset. To test each domain, we used a leave-one-out setting, where three domains are used as meta-train domains and the remaining domain as the meta-test domain. This setup allows us to measure how well the model generalizes object quantification to unseen domains by training with textual descriptions from the other three domains.

Metrics. To evaluate quantification accuracy, we use the

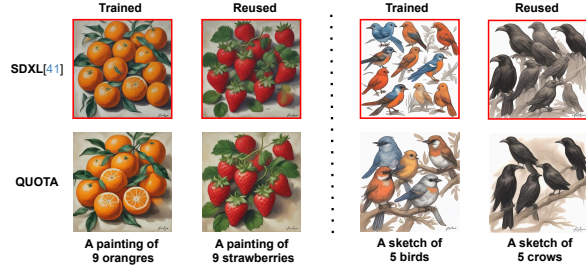


Figure 4. Generalization to unseen classes. Comparison of object quantification and style consistency between stable diffusion and our QUOTA, on both trained and unseen (reused) classes. While SDXL [41] struggles with unseen classes, QUOTA accurately controls object quantification and maintains semantic alignment across both trained classes (e.g., oranges, birds) and unseen classes (e.g., strawberries, crows). This demonstrates the robustness of QUOTA in adapting to previously unseen classes and domains.

MAE (Mean Absolute Error) and RMSE (Root Mean Square Error) metrics based on YOLOv9 [62]. These metrics are calculated by comparing the detected object counts to the target count in each image, with MAE capturing the average absolute deviation and RMSE highlighting larger errors through squared deviations. For semantic alignment assessment, we use a normalized CLIP matching score, defined as $CLIP-S(p, x_d) = w \cdot \max(\cos(p, x_d), 0)$, where p is the prompt and x_d is the generated image [18]. Lastly, we calculate the average performance across different domains to assess each model’s consistency and adaptability to diverse contexts.

Implementation Details. We conducted training and evaluation on a single NVIDIA A6000 GPU with 48GB of memory. Training each token requires approximately two minutes, totaling around 30 iterations, using the SDXL framework [41]. For image quality, we find that a single denoising step is sufficient. The optimized quantification token can be reused without additional optimization time. We set $\lambda=5$, a learning rate of 0.01 for optimization, and the clipcount scaling hyperparameter λ_{scale} to 60 for a static scale. We will make our code available.

Baselines. We establish a baseline using SDXL [41] backbone. We also compare with IoCo [66], which learns the quantification token only during training and considers im-

	Photo			Painting			Cartoon			Sketch			Average		
	YOLO		CLIP-S \uparrow	YOLO		CLIP-S \uparrow	YOLO		CLIP-S \uparrow	YOLO		CLIP-S \uparrow	YOLO	CLIP-S \uparrow	
	MAE \downarrow	RMSE \downarrow		MAE \downarrow	RMSE \downarrow		MAE \downarrow	RMSE \downarrow		MAE \downarrow	RMSE \downarrow		MAE \downarrow	RMSE \downarrow	
SDXL [41]	14.77	20.26	73.2	12.27	17.17	73.5	14.10	17.97	72.5	11.92	16.51	71.4	13.26	17.98	72.7
w/ e_{style}	14.41	19.26	73.3	11.31	15.28	73.7	12.73	15.07	72.9	9.91	13.25	72.7	12.28	16.15	73.2
w/ e_{count}	14.12	19.60	73.9	10.20	14.44	74.1	10.66	13.17	73.7	8.75	11.89	73.3	10.94	14.76	73.8
Ours (w/ e_{count} & e_{style})	10.09	13.98	74.3	8.04	11.04	75.9	9.48	11.92	74.8	9.15	11.69	74.1	9.19	12.16	74.8

Table 2. Impact of learnable tokens on object quantification and semantic alignment across different domains on the FSC benchmark. Adding learnable tokens e_{count} and e_{style} improves YOLO-based MAE, RMSE, and CLIP-S scores, with the best performance achieved when both tokens are used together.

	Photo			Painting			Cartoon			Sketch			Average		
	YOLO		CLIP-S \uparrow	YOLO		CLIP-S \uparrow	YOLO		CLIP-S \uparrow	YOLO		CLIP-S \uparrow	YOLO	CLIP-S \uparrow	
	MAE \downarrow	RMSE \downarrow		MAE \downarrow	RMSE \downarrow		MAE \downarrow	RMSE \downarrow		MAE \downarrow	RMSE \downarrow		MAE \downarrow	RMSE \downarrow	
SDXL [41]	14.77	20.26	73.2	12.27	17.17	73.5	14.10	17.97	72.5	11.92	16.51	71.4	13.26	17.98	72.7
Only train domains	12.75	16.75	73.2	10.40	13.78	74.0	11.49	13.28	73.1	11.33	12.92	71.9	11.49	14.18	73.1
IoCo [66]	7.72	12.21	74.4	11.36	15.68	73.1	12.40	15.93	72.7	10.80	14.21	71.9	10.57	14.51	73.0
QUOTA	10.09	13.98	74.3	8.04	11.04	75.9	9.48	11.92	74.8	9.15	11.69	74.1	9.19	12.16	74.8
Only test domain	5.68	8.63	75.9	4.61	7.12	76.8	5.31	7.86	75.9	5.94	8.53	75.3	5.38	8.04	76.0
Train domains & Test domain	6.43	9.05	74.7	7.61	10.79	76.1	8.43	10.96	75.1	8.75	11.27	74.7	7.81	10.52	75.2

Table 3. Performance comparison with various baseline models on object quantification and semantic alignment across different domains on the FSC benchmark. The methods and numbers shown in gray represent the upper bound, as these models have been trained using the test domain. Note that IoCo [66] is specifically trained on the Photo, which explains its high performance on Photo. In contrast, our QUOTA achieves strong results across all domains without having been explicitly trained on Photo, highlighting its domain-generalizable capabilities.

ages in the Photo domain exclusively.

5.2. Results

Benefit of meta-optimization. Table 1 demonstrates the impact of meta-optimization on object quantification accuracy and semantic alignment across different image styles. On average, meta-optimization achieves substantial improvements in both MAE and RMSE, highlighting enhanced object quantification accuracy and adaptability. The benefits are particularly pronounced in challenging domains, such as Cartoon, where meta-optimization leads to improved precision and consistency. Additionally, meta-optimization improves semantic alignment, as indicated by higher CLIP-S scores, reflecting closer alignment with prompt semantics. Figure 3 provides qualitative examples, comparing outputs from stable diffusion, an inner-loop-only optimization, and our full QUOTA framework. While inner-loop-only optimization offers some gains, it still struggles with consistent counts. In contrast, our complete meta-optimization approach, which includes both inner and outer loops, enables precise and domain-invariant object quantification across all styles, even in difficult cases like Sketch. These results confirm that meta-optimization significantly enhances the model’s ability to generalize quantification and semantic consistency across diverse domains.

Benefit of learnable tokens. Table 2 demonstrates the impact of adding learnable tokens e_{count} and e_{style} on object quantification accuracy and semantic alignment across different domains. The standard stable diffusion model, without any learnable tokens, shows limited adaptability, achieving lower accuracy across all domains. Introducing the

e_{style} token alone provides moderate improvements, indicating that adapting to domain style contributes positively to performance. Adding only the e_{count} token leads to further enhancements, emphasizing the importance of object count adaptation. When both learnable tokens e_{count} and e_{style} are combined, as in QUOTA, the model achieves the best performance across all metrics and domains. This setup consistently enhances both counting accuracy and domain adaptability, highlighting the complementary effects of using both tokens. These results confirm that the joint use of e_{count} and e_{style} significantly strengthens the model’s ability to generalize object quantification across diverse domains while maintaining robust semantic alignment.

Generalization on unseen classes. In this experiment, we demonstrate the ability of our model, trained on 19 predefined classes, to generalize effectively to unseen classes using the optimized prompts generated by QUOTA. As illustrated in Figure 4, we tested the model on new classes not encountered during training, such as *strawberries* and *crows*. This generalization capability arises from our dual-loop training approach, where both the inner and outer loops are exposed to different domains and classes. By alternating between meta-train and meta-test domains with varying classes in each loop, our framework mimics the testing scenario of unseen class predictions, preparing the model for diverse and previously unseen content. Our approach successfully adapts to both the unseen classes and their respective domains, accurately controlling the object quantification and preserving semantic alignment. These results highlight QUOTA’s robustness in generalizing object quantification and domain consistency to new classes, demonstrating its potential for

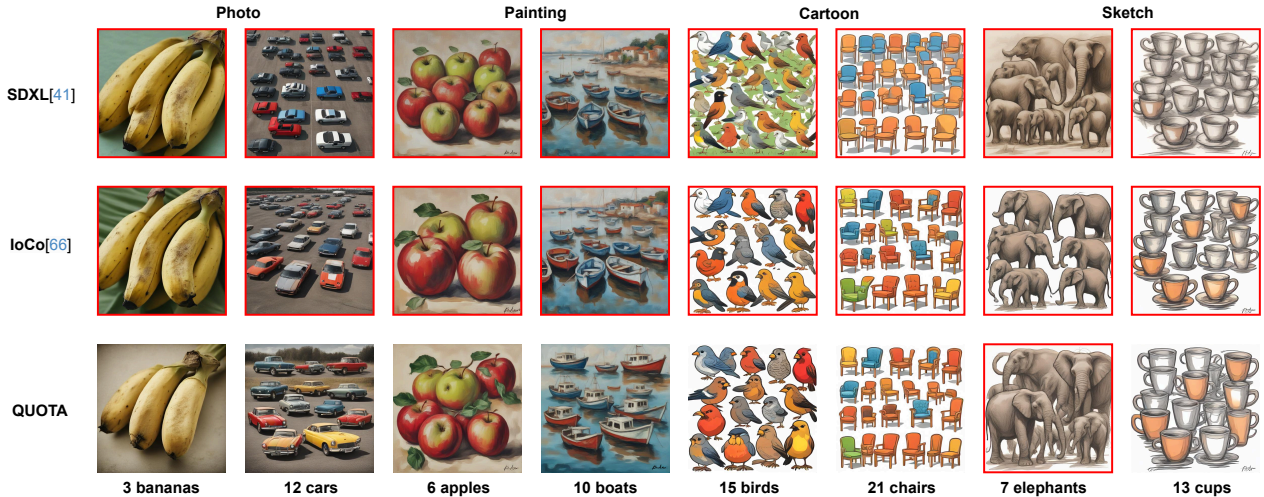


Figure 5. Qualitative comparison of generated images across different domains and classes. This comparison highlights the superior quantification accuracy and domain consistency achieved by QUOTA across diverse domains. The images outlined in red represent cases where the generated images have incorrect object quantification. The box in the Sketch domain showcases a challenging failure case for QUOTA, emphasizing the difficulty of accurately quantifying objects in highly stylized and intricate settings.

broad applicability in diverse scenarios.

Comparison with different baselines. To provide a comprehensive understanding of QUOTA’s performance, we include a qualitative comparison in Figure 5 alongside the quantitative results in Table 3. Figure 5 illustrates generated images across various domains and classes, with QUOTA demonstrating superior quantification accuracy and domain consistency. In contrast, SDXL [41] and IoCo [66] struggle with incorrect object quantification across different domains, as indicated by the red outlines on images with quantification errors. QUOTA achieves consistent object counts close to the target quantities in most cases, while the baseline models frequently misestimate counts, especially in complex domains. Notably, IoCo’s reliance on training within the photo domain explains its higher performance in this domain but highlights its limitations in generalizing to unseen styles. The highlighted box in the Sketch domain shows a failure case for QUOTA, emphasizing the challenges in accurately quantifying objects within highly stylized and intricate settings. Together, these visual and numerical comparisons underscore QUOTA’s capability to set a new benchmark for object quantification accuracy and domain adaptability in text-to-image generation.

Limitations and Future Work. While our approach demonstrates robust performance across various domains, it has limitations in particularly challenging domains, where improvements are less pronounced. This may be due to the inherent difficulty of accurately quantifying objects in abstract or highly stylized representations, although our method still outperforms previous approaches in these cases. Additionally, the use of a dual-loop meta-learning strategy introduces a higher computational cost during training, as it requires

more iterations for optimizing domain-invariant prompts. However, at test time, our approach remains faster than traditional adaptation-based methods, such as IoCo [66], which require additional adaptation steps.

For future work, we plan to explore alternative object detectors to improve object quantification accuracy in challenging domains. Additionally, our method could be extended to other text-to-image generation models and applied to different tasks, such as fine-grained attribute control and scene layout generation, broadening its applicability within generative modeling.

6. Conclusion

In this work, we presented QUOTA, a novel optimization framework for domain-agnostic object quantification in generative text-to-image models. Unlike existing methods that require retraining for each new domain, QUOTA enables accurate object quantification across diverse and unseen domains through a dual-loop meta-learning strategy that optimizes a domain-invariant prompt. By integrating learnable quantification and domain tokens within prompt learning, our approach captures stylistic variations and maintains accuracy, even for object classes not seen during training. We introduced a new benchmark specifically for evaluating domain-generalizable object quantification, allowing rigorous assessment of model adaptability and quantification accuracy across domains. Extensive experiments demonstrate that QUOTA outperforms conventional models in both object quantification accuracy and semantic consistency, setting a new standard for efficient, scalable, and flexible text-to-image generation across any domain.

7. Acknowledgment

This work is financially supported by the Inception Institute of Artificial Intelligence, the University of Amsterdam, the Cisco gift funding, and the allowance Top consortia for Knowledge and Innovation (TKIs) from the Netherlands Ministry of Economic Affairs and Climate Policy.

References

- [1] Antreas Antoniou, Harrison Edwards, and Amos Storkey. How to train your maml. In *ICLR*, 2019. 3
- [2] Yogesh Balaji, Swami Sankaranarayanan, and Rama Chellappa. Metareg: Towards domain generalization using meta-regularization. In *NeurIPS*, 2018. 3
- [3] Sarah Bechtel, Artem Molchanov, Yevgen Chebotar, Edward Grefenstette, Ludovic Righetti, Gaurav S. Sukhatme, and Franziska Meier. Meta learning via learned loss. In *ICPR*, 2020. 3
- [4] Fabio M Carlucci, Antonio D’Innocente, Silvia Bucci, Barbara Caputo, and Tatiana Tommasi. Domain generalization by solving jigsaw puzzles. In *CVPR*, pages 2229–2238, 2019. 2
- [5] Hila Chefer, Yuval Alaluf, Yael Vinker, Lior Wolf, and Daniel Cohen-Or. Attend-and-excite: Attention-based semantic guidance for text-to-image diffusion models. *TOG*, 42(4):1–10, 2023. 2
- [6] Katherine Crowson, Stella Biderman, Daniel Kornis, Dashiell Stander, Eric Hallahan, Louis Castricato, and Edward Raff. VQGAN-CLIP: Open Domain Image Generation and Editing with Natural Language Guidance. In *ECCV*, pages 88–105, Cham, 2022. Springer Nature Switzerland. 2
- [7] Quan Dao, Hao Phung, Binh Nguyen, and Anh Tran. Flow matching in latent space. *arXiv preprint arXiv:2307.08698*, 2023. 1
- [8] Ming Ding, Wendi Zheng, Wenyi Hong, and Jie Tang. Cogview2: Faster and better text-to-image generation via hierarchical transformers. *arXiv preprint arXiv:2204.14217*, 2022. 2
- [9] Yingjun Du, Jun Xu, Huan Xiong, Qiang Qiu, Xiantong Zhen, Cees GM Snoek, and Ling Shao. Learning to learn with variational information bottleneck for domain generalization. In *ECCV*, pages 200–216. Springer, 2020. 1, 2, 3
- [10] Yingjun Du, Xiantong Zhen, Ling Shao, and Cees G M Snoek. Hierarchical variational memory for few-shot learning across domains. In *ICLR*, 2022. 3
- [11] Yingjun Du, Jiayi Shen, Xiantong Zhen, and Cees GM Snoek. Emo: episodic memory optimization for few-shot meta-learning. In *CoLLAs*, pages 1–20. PMLR, 2023. 3
- [12] Chelsea Finn, Pieter Abbeel, and Sergey Levine. Model-agnostic meta-learning for fast adaptation of deep networks. In *ICML*, pages 1126–1135. JMLR. org, 2017. 2, 3
- [13] Oran Gafni, Adam Polyak, Oron Ashual, Shelly Sheynin, Devi Parikh, and Yaniv Taigman. Make-A-Scene: Scene-Based Text-to-Image Generation with Human Priors. In *ECCV*, pages 89–106, Cham, 2022. Springer Nature Switzerland. 2
- [14] Rinon Gal, Yuval Alaluf, Yuval Atzmon, Or Patashnik, Amit Haim Bermano, Gal Chechik, and Daniel Cohen-or. An image is worth one word: Personalizing text-to-image generation using textual inversion. In *ICLR*, 2023. 2
- [15] Ian Goodfellow, Jean Pouget-Abadie, Mehdi Mirza, Bing Xu, David Warde-Farley, Sherjil Ozair, Aaron Courville, and Yoshua Bengio. Generative adversarial nets. *NeurIPS*, 27, 2014. 2
- [16] Erin Grant, Chelsea Finn, Sergey Levine, Trevor Darrell, and Thomas Griffiths. Recasting gradient-based meta-learning as hierarchical bayes. In *ICLR*, 2018. 3
- [17] Amir Hertz, Ron Mokady, Jay Tenenbaum, Kfir Aberman, Yael Pritch, and Daniel Cohen-or. Prompt-to-Prompt Image Editing with Cross-Attention Control. In *ICLR*, 2023. 2
- [18] Jack Hessel, Ari Holtzman, Maxwell Forbes, Ronan Le Bras, and Yejin Choi. Clipscore: A reference-free evaluation metric for image captioning. *arXiv preprint arXiv:2104.08718*, 2021. 6
- [19] Jonathan Ho, Ajay Jain, and Pieter Abbeel. Denoising diffusion probabilistic models. *NeurIPS*, 33:6840–6851, 2020. 2
- [20] Sepp Hochreiter, A Steven Younger, and Peter R Conwell. Learning to learn using gradient descent. In *ICANN*, 2001. 2, 3
- [21] Timothy Hospedales, Antreas Antoniou, Paul Micaelli, and Amos Storkey. Meta-learning in neural networks: A survey. *TPAMI*, 44(9):5149–5169, 2021. 3
- [22] Dasol Hwang, Jinyoung Park, Sunyoung Kwon, KyungMin Kim, Jung-Woo Ha, and Hyunwoo J Kim. Self-supervised auxiliary learning with meta-paths for heterogeneous graphs. In *NeurIPS*, 2020. 3
- [23] Dasol Hwang, Jinyoung Park, Sunyoung Kwon, KyungMin Kim, Jung-Woo Ha, and Hyunwoo J Kim. Self-supervised auxiliary learning for graph neural networks via meta-learning. *arXiv:2103.00771*, 2021. 3
- [24] Ajay Jain, Ben Mildenhall, Jonathan T Barron, Pieter Abbeel, and Ben Poole. Zero-shot text-guided object generation with dream fields. In *CVPR*, pages 867–876, 2022. 2
- [25] Yunpei Jia, Jie Zhang, Shiguang Shan, and Xilin Chen. Single-side domain generalization for face anti-spoofing. In *CVPR*, pages 8484–8493, 2020. 2
- [26] Daehee Kim, Youngjun Yoo, Seunghyun Park, Jinkyu Kim, and Jaekoo Lee. Selfreg: Self-supervised contrastive regularization for domain generalization. In *ICCV*, pages 9619–9628, 2021. 2
- [27] Dohwan Ko, Joonmyung Choi, Hyeong Kyu Choi, KyoungWoon On, Byungseok Roh, and Hyunwoo J Kim. Meltr: Meta loss transformer for learning to fine-tune video foundation models. In *CVPR*, 2023. 3
- [28] Gregory Koch. Siamese neural networks for one-shot image recognition. In *ICML Workshop*, 2015. 3
- [29] Kwonjoon Lee, Subhansu Maji, Avinash Ravichandran, and Stefano Soatto. Meta-learning with differentiable convex optimization. In *CVPR*, 2019. 3
- [30] Bowen Li, Xiaojuan Qi, Thomas Lukasiewicz, and Philip Torr. Controllable text-to-image generation. *NeurIPS*, 32, 2019. 2

- [31] Da Li, Yongxin Yang, Yi-Zhe Song, and Timothy Hospedales. Learning to generalize: Meta-learning for domain generalization. In *AAAI*, 2018. 1, 3
- [32] Haoliang Li, Sinno Jialin Pan, Shiqi Wang, and Alex C Kot. Domain generalization with adversarial feature learning. In *CVPR*, pages 5400–5409, 2018. 2
- [33] Haoliang Li, YuFei Wang, Renjie Wan, Shiqi Wang, Tie-Qiang Li, and Alex Kot. Domain generalization for medical imaging classification with linear-dependency regularization. *NeurIPS*, 33:3118–3129, 2020. 2
- [34] Wenbo Li, Pengchuan Zhang, Lei Zhang, Qiuyuan Huang, Xiaodong He, Siwei Lyu, and Jianfeng Gao. Object-driven text-to-image synthesis via adversarial training. In *CVPR*, pages 12174–12182, 2019. 2
- [35] Nikhil Mishra, Mostafa Rohaninejad, Xi Chen, and Pieter Abbeel. A simple neural attentive meta-learner. In *ICLR*, 2018. 3
- [36] Ron Mokady, Amir Hertz, Kfir Aberman, Yael Pritch, and Daniel Cohen-Or. Null-text inversion for editing real images using guided diffusion models. In *CVPR*, pages 6038–6047, 2023. 2
- [37] Tsendsuren Munkhdalai and Hong Yu. Meta networks. In *ICML*, 2017. 3
- [38] Tsendsuren Munkhdalai, Xingdi Yuan, Soroush Mehri, and Adam Trischler. Rapid adaptation with conditionally shifted neurons. In *ICML*, 2018. 3
- [39] Alex Nichol, Joshua Achiam, and John Schulman. On first-order meta-learning algorithms. *arXiv:1803.02999*, 2018. 3
- [40] Roni Paiss, Ariel Ephrat, Omer Tov, Shiran Zada, Inbar Mosseri, Michal Irani, and Tali Dekel. Teaching clip to count to ten. In *ICCV*, pages 3170–3180, 2023. 1
- [41] Dustin Podell, Zion English, Kyle Lacey, Andreas Blattmann, Tim Dockhorn, Jonas Müller, Joe Penna, and Robin Rombach. Sdxl: Improving latent diffusion models for high-resolution image synthesis. *arXiv preprint arXiv:2307.01952*, 2023. 1, 3, 4, 5, 6, 7, 8, 11, 12
- [42] Tingting Qiao, Jing Zhang, Duanqing Xu, and Dacheng Tao. Learn, imagine and create: Text-to-image generation from prior knowledge. *NeurIPS*, 32, 2019. 2
- [43] Tingting Qiao, Jing Zhang, Duanqing Xu, and Dacheng Tao. Mirrorgan: Learning text-to-image generation by redescription. In *CVPR*, pages 1505–1514, 2019. 2
- [44] Alec Radford, Jong Wook Kim, Chris Hallacy, Aditya Ramesh, Gabriel Goh, Sandhini Agarwal, Girish Sastry, Amanda Askell, Pamela Mishkin, and Jack Clark. Learning transferable visual models from natural language supervision. In *ICML*, 2021. 4
- [45] Aditya Ramesh, Mikhail Pavlov, Gabriel Goh, Scott Gray, Chelsea Voss, Alec Radford, Mark Chen, and Ilya Sutskever. Zero-shot text-to-image generation. In *ICML*, pages 8821–8831. PMLR, 2021. 2
- [46] Aditya Ramesh, Prafulla Dhariwal, Alex Nichol, Casey Chu, and Mark Chen. Hierarchical text-conditional image generation with clip latents, 2022. 2
- [47] Viresh Ranjan, Udbhav Sharma, Thu Nguyen, and Minh Hoai. Learning to count everything. In *CVPR*, pages 3394–3403, 2021. 6
- [48] Sachin Ravi and Hugo Larochelle. Optimization as a model for few-shot learning. In *ICLR*, 2016. 3
- [49] Robin Rombach, Andreas Blattmann, Dominik Lorenz, Patrick Esser, and Björn Ommer. High-resolution image synthesis with latent diffusion models. In *CVPR*, pages 10684–10695, 2022. 2
- [50] Nataniel Ruiz, Yuanzhen Li, Varun Jampani, Yael Pritch, Michael Rubinstein, and Kfir Aberman. Dreambooth: Fine tuning text-to-image diffusion models for subject-driven generation. In *CVPR*, 2023. 2
- [51] Chitwan Saharia, William Chan, Saurabh Saxena, Lala Li, Jay Whang, Emily Denton, Seyed Kamyar Seyed Ghasemipour, Raphael Gontijo-Lopes, Burcu Karagol Ayan, Tim Salimans, Jonathan Ho, David J. Fleet, and Mohammad Norouzi. Photorealistic Text-to-Image Diffusion Models with Deep Language Understanding. In *NeurIPS*, 2022. 2
- [52] Adam Santoro, Sergey Bartunov, Matthew Botvinick, Daan Wierstra, and Timothy Lillicrap. Meta-learning with memory-augmented neural networks. In *ICML*, pages 1842–1850, 2016. 3
- [53] Rui Shao, Xiangyuan Lan, Jiawei Li, and Pong C Yuen. Multi-adversarial discriminative deep domain generalization for face presentation attack detection. In *CVPR*, pages 10023–10031, 2019. 2
- [54] Jun Shu, Qi Xie, Lixuan Yi, Qian Zhao, Sanping Zhou, Zongben Xu, and Deyu Meng. Meta-weight-net: Learning an explicit mapping for sample weighting. In *NeurIPS*, 2019. 3
- [55] Yang Shu, Zhangjie Cao, Chenyu Wang, Jianmin Wang, and Mingsheng Long. Open domain generalization with domain-augmented meta-learning. In *CVPR*, pages 9624–9633, 2021. 2
- [56] Jake Snell, Kevin Swersky, and Richard Zemel. Prototypical networks for few-shot learning. In *NeurIPS*, pages 4077–4087, 2017. 3
- [57] Ariel Starr, Melissa E Libertus, and Elizabeth M Brannon. Number sense in infancy predicts mathematical abilities in childhood. *NAS*, 110(45):18116–18120, 2013. 1
- [58] Flood Sung, Yongxin Yang, Li Zhang, Tao Xiang, Philip HS Torr, and Timothy M Hospedales. Learning to compare: Relation network for few-shot learning. In *CVPR*, pages 1199–1208, 2018. 3
- [59] Ming Tao, Hao Tang, Fei Wu, Xiao-Yuan Jing, Bing-Kun Bao, and Changsheng Xu. DF-GAN: A Simple and Effective Baseline for Text-to-Image Synthesis. In *CVPR*, pages 16515–16525, 2022. 2
- [60] Sebastian Thrun and Lorien Pratt. *Learning to learn*. Springer Science & Business Media, 2012. 2
- [61] Oriol Vinyals, Charles Blundell, Timothy Lillicrap, and Daan Wierstra. Matching networks for one shot learning. In *NeurIPS*, pages 3630–3638, 2016. 3
- [62] Chien-Yao Wang, I-Hau Yeh, and Hong-Yuan Mark Liao. Yolov9: Learning what you want to learn using programmable gradient information, 2024. 4, 6
- [63] Zehao Xiao, Jiayi Shen, Xiantong Zhen, Ling Shao, and Cees Snoek. A bit more bayesian: Domain-invariant learning with uncertainty. In *ICML*, pages 11351–11361. PMLR, 2021. 1

- [64] Huaxiu Yao, Linjun Zhang, and Chelsea Finn. Meta-learning with fewer tasks through task interpolation. *arXiv preprint arXiv:2106.02695*, 2021. 3
- [65] Jiahui Yu, Yuanzhong Xu, Jing Yu Koh, Thang Luong, Gunjan Baid, Zirui Wang, Vijay Vasudevan, Alexander Ku, Yinfei Yang, Burcu Karagol Ayan, Ben Hutchinson, Wei Han, Zarana Parekh, Xin Li, Han Zhang, Jason Baldridge, and Yonghui Wu. Scaling Autoregressive Models for Content-Rich Text-to-Image Generation. *TMLR*, 2022. Featured Certification. 2
- [66] Oz Zafar, Lior Wolf, and Idan Schwartz. Iterative object count optimization for text-to-image diffusion models. *arXiv preprint arXiv:2408.11721*, 2024. 1, 3, 6, 7, 8, 11, 12
- [67] Yan Zhang, Jonathon Hare, and Adam Prügel-Bennett. Learning to count objects in natural images for visual question answering. *arXiv preprint arXiv:1802.05766*, 2018. 1
- [68] Zizhao Zhang, Yuanpu Xie, and Lin Yang. Photographic text-to-image synthesis with a hierarchically-nested adversarial network. In *CVPR*, pages 6199–6208, 2018. 2
- [69] Luisa Zintgraf, Kyriacos Shiarli, Vitaly Kurin, Katja Hofmann, and Shimon Whiteson. Fast context adaptation via meta-learning. In *ICML*, pages 7693–7702, 2019. 3

8. Appendix

8.1. Performance Across Object Quantities

Table 4 and Table 5 present the Mean Absolute Error (MAE) results for 19 categories under two test domains: *Painting* and *Cartoon*, evaluating object quantities ranging from 1 to 25. The results provide a fine-grained comparison between SDXL [41], IoCo [66], and our method QUOTA. In the *Painting* domain, our method achieves the best performance in 20 out of 25 quantities, significantly surpassing both IoCo and SDXL, while in the *Cartoon* domain, QUOTA ranks first in 19 out of 25 quantities, demonstrating its robustness in handling the challenges of stylized visual representations. These results underline the consistent superiority of QUOTA in capturing complex visual variations and maintaining accurate counting performance across diverse object categories and quantities, further highlighting its effectiveness in real-world scenarios requiring precise object quantification.

8.2. Quantitative Evaluation on Unseen Classes

Table 6 presents a detailed quantitative analysis of object quantification performance on unseen classes across different test domains. The unseen classes are grouped based on their semantic similarities to the trained categories (e.g., apples generalize to tomatoes, oranges, and strawberries; birds generalize to crows, pigeons, and seagulls; and sheep generalize to zebras, horses, and cows). The metrics include MAE, RMSE, and CLIP-S scores. MAE and RMSE, averaged over nine unseen classes and from 1 to 25 object amounts, evaluate quantification accuracy, while higher CLIP-S scores indicate better semantic alignment. Our method QUOTA consistently outperforms both SDXL [41] and IoCo [66] across

all test domains, including *Photo*, *Painting*, *Cartoon*, and *Sketch*. Specifically, QUOTA achieves significantly lower MAE and RMSE compared to both baselines, demonstrating its superior quantification accuracy. Additionally, QUOTA achieves higher CLIP-S scores, indicating better semantic alignment and generalization to unseen classes. These results underline the robustness and adaptability of QUOTA in handling diverse test domains and unseen class distributions, outperforming state-of-the-art baselines across all evaluated metrics.

8.3. Robust Generalization to Unseen Classes

As shown in Figure 6, we train the models on the class ‘apples’ in the painting test domain and evaluate their generalization performance on semantically related but unseen classes: ‘tomatoes’, ‘oranges’, and ‘strawberries’. While IoCo [66] performs well on the trained class during training, it completely fails to generalize to unseen classes, resulting in inaccurate quantification across all tested categories. Similarly, SDXL [41] struggles to adapt, with inconsistent object counts and poor alignment with the prompts. In contrast, our method QUOTA demonstrates robust generalization, achieving accurate object quantification across all unseen categories. This highlights QUOTA’s ability to adapt to previously unseen classes and maintain reliable performance, even in domains that are stylistically distinct from the training set. These results underscore the superiority of QUOTA in addressing the challenges of cross-domain and cross-class generalization.

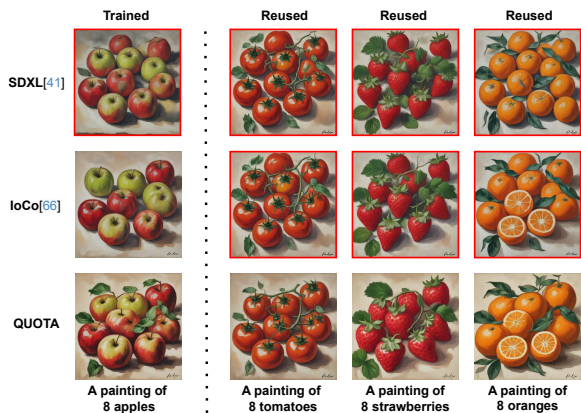


Figure 6. Additional results on generalization to unseen classes. Comparison of object quantification between SDXL [41], IoCo [66], and our QUOTA, evaluated on both trained and unseen (reused) classes.

Models	1	2	3	4	5	6	7	8	9	10	11	12	13
SDXL [41]	2.33	1.47	3.20	5.33	5.60	8.33	8.6	9.73	11.33	15.33	14.00	16.60	14.53
IoCo [66]	3.67	1.53	2.40	3.93	6.73	7.93	9.07	9.77	8.53	14.33	15.00	11.67	12.67
QUOTA	2.20	2.00	3.00	3.67	4.40	6.01	6.80	9.07	6.47	7.00	6.47	7.33	8.13
Models	14	15	16	17	18	19	20	21	22	23	24	25	Avg
SDXL [41]	17.33	17.87	16.00	17.67	15.13	16.67	11.93	15.00	13.13	15.80	16.93	17.00	12.27
IoCo [66]	15.07	17.40	14.67	14.80	15.47	15.87	13.40	15.27	12.93	12.87	15.80	13.33	11.36
QUOTA	8.87	9.60	7.80	7.47	9.27	9.67	10.47	12.47	14.20	14.13	10.53	14.07	8.04

Table 4. MAE comparison across 19 categories in the *Painting* test domain for varying object amounts. This table evaluates SDXL [41], IoCo [66], and QUOTA on object quantification for amounts ranging from 1 to 25, averaged across 19 categories in the *Painting* test domain. QUOTA achieves the best performance in 20 out of 25 quantities, highlighting its superior accuracy and robustness in this test domain.

Models	1	2	3	4	5	6	7	8	9	10	11	12	13
SDXL [41]	3.80	1.13	2.93	3.27	6.47	8.53	8.07	13.40	12.80	16.53	17.73	16.63	17.60
IoCo [66]	7.20	1.93	3.20	3.60	6.40	8.00	9.33	12.60	12.00	14.27	16.13	12.67	16.80
QUOTA	2.80	1.53	3.40	5.27	6.33	5.73	7.27	8.13	9.47	13.13	9.60	10.27	10.40
Models	14	15	16	17	18	19	20	21	22	23	24	25	Avg
SDXL [41]	18.00	18.53	17.27	17.47	17.00	20.20	18.80	17.20	18.13	17.93	18.87	24.47	14.10
IoCo [66]	14.27	15.87	17.40	18.20	16.27	12.87	17.07	12.73	13.87	14.73	14.47	18.13	12.40
QUOTA	15.00	10.00	11.87	8.80	7.80	9.13	13.87	13.40	15.60	11.13	12.67	14.60	9.48

Table 5. MAE comparison across 19 categories in the *cartoon* test domain for varying object amounts. This table evaluates SDXL [41], IoCo [66], and QUOTA on object quantification for amounts ranging from 1 to 25, averaged across 19 categories in the *cartoon* test domain. QUOTA achieves the best performance in 19 out of 25 quantities, highlighting its superior accuracy and robustness in this test domain.

	Photo		Painting		Cartoon		Sketch		Average						
	YOLO	CLIP-S \uparrow	YOLO	CLIP-S \uparrow	YOLO	CLIP-S \uparrow	YOLO	CLIP-S \uparrow	YOLO	CLIP-S \uparrow					
	MAE \downarrow	RMSE \downarrow	MAE \downarrow	RMSE \downarrow	MAE \downarrow	RMSE \downarrow	MAE \downarrow	RMSE \downarrow	MAE \downarrow	RMSE \downarrow					
SDXL [41]	14.07	19.80	72.8	20.64	27.05	73.0	11.71	15.40	72.1	18.39	24.03	71.1	16.20	21.57	72.3
IoCo [66]	13.42	18.97	73.3	13.16	19.01	73.4	11.29	14.73	72.7	14.41	19.71	71.60	13.07	18.11	72.8
QUOTA	13.72	19.20	73.1	10.99	15.24	74.5	9.94	12.22	73.2	12.05	14.68	72.3	11.68	15.33	73.3

Table 6. Quantitative evaluation of generalization to unseen classes through object quantification across diverse domains. This table provides a detailed analysis of object quantification with various baseline models across four test domains: *Photo*, *Painting*, *Cartoon*, and *Sketch*. While SDXL [41] exhibits higher errors across all domains, and IoCo [66] achieves competitive performance specifically on *Photo* due to being explicitly trained on this domain, QUOTA consistently achieves lower MAE and RMSE values as well as higher CLIP-S scores across all test domains. This demonstrates QUOTA’s superior ability to accurately quantify object amounts, maintain strong semantic alignment, and adapt to unseen categories, even in stylistically distinct and challenging domains.